ResearchGate

See discussions, stats, and author profiles for this publication at: https://www.researchgate.net/publication/258033868

Thermal Response of DNA Supramolecular Polymers Assembled with Hydrophobic Sticky Ends

ARTICLE *in* THE JOURNAL OF PHYSICAL CHEMISTRY B · OCTOBER 2013

Impact Factor: 3.3 · DOI: 10.1021/jp4087078 · Source: PubMed

READS

24

4 AUTHORS, INCLUDING:

Mahesh Hariharan

Indian Institute Of Science Education and Res…

45 PUBLICATIONS **834** CITATIONS

SEE PROFILE

Frederick D Lewis

Northwestern University

320 PUBLICATIONS **9,152** CITATIONS

SEE PROFILE

Available from: Mahesh Hariharan

Retrieved on: 16 January 2016

THE JOURNAL OF PHYSICAL CHEMISTRY B

Article

pubs.acs.org/JPCB

Thermal Response of DNA Supramolecular Polymers Assembled with Hydrophobic Sticky Ends

Mahesh Hariharan,*[,†,‡] Yan Zheng,[†] Boris Rybtchinski,*[,§] and Frederick D. Lewis*[,†]

[†]Department of Chemistry, Northwestern University, Evanston, Illinois 60208-3113, United States

[‡]School of Chemistry, Indian Institute of Science Education and Research Thiruvananthapuram (IISER TVM), Thiruvananthapuram, Kerala, India 695 016

[§]Department of Organic Chemistry, Weizmann Institute of Science, Rehovot 76100, Israel

Supporting Information

ABSTRACT: We report the self-assembly and thermal dissociation of DNA dumbbell conjugates having a perylenediimide (PDI) linker on each end separated by 6−16 A−T base pairs. In the presence of NaCl these dumbbells form one-dimensional supramolecular assemblies as a consequence of the hydrophobic association of their PDI sticky ends. The dependence of assembly formation on dumbbell concentration, salt concentration, and temperature can be conveniently monitored by UV−vis spectroscopy. The melting of these linear assemblies follows two limiting mechanisms, depending on the length of the dumbbells. Upon heating in the presence of salt, the assemblies formed by the longer dumbbells undergo a sequential transition from assembly to base-paired monomer to random coiled monomer, whereas the assemblies formed by the shorter dumbbells undergo disassembly and base-pair melting cooperatively. In all cases, the intramolecular hydrophobic association of the PDI chromophores is observed at elevated temperature. The thermal behavior of these one-dimensional assemblies is compared to that of other sticky-ended assemblies.

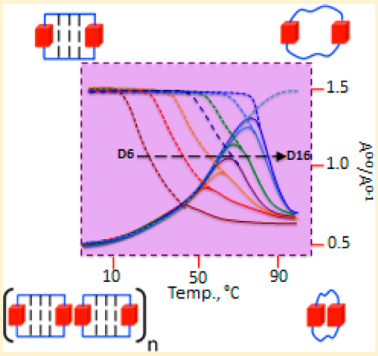

INTRODUCTION

DNA has proven to be a highly versatile biopolymer for the construction of a wide range of one-, two-, and three-dimensional structures.[1−3] Understanding the principles of DNA-programmed assembly of nanostructures has long been the principle focus of this field.[4,5] The connection of DNA-based hybrid systems using the "sticky end" approach has been the dominant mode of formation for 1-D and higher order assemblies.[6] Metal ion-mediated assembly,[7] hydrophobic association of perylenediimides,[8] clustering of cationic stilbazoles,[9] and adamantane-β-cyclodextrin complexation[10] have been employed as alternate methods of 1-D DNA assembly. Further functionalization of nanoparticles, biological, and organic molecules on the exterior of a linear DNA scaffold[11] can lead to the generation of well-defined 1-D nanoarchitectures.[12]

Recently the thermal response of DNA nanostructures has received increasing attention, not only in order to better understand the kinetics and thermodynamics of nanostructure formation and disassembly, but also for applications such as cargo release.[13,14] Using fluorescence resonance energy transfer (FRET), Liu and co-workers have investigated the effects of local and long-range structural defects on the thermal stability of 2-D and 3-D DNA origami in solution.[15] The direct visualization of the intermediary stages in the thermal reorganization of the DNA origami at the solid−liquid interface has also been carried out by Dong and co-workers[16] using atomic force microscopy. Thermal stability also plays a crucial role in the formation of 1-D DNA aggregates[1] that have potential applications in molecular electronics,[3] catalysis,[13] and templated formation of organic-,[17] bio-,[18,19] and nanoassemblies. Understanding the competitive thermodynamic stability[15,16] of the sticky end that holds the assembly together versus the cooperative interactions that form the DNA duplex could provide the mechanistic insight needed to optimize the formation and/or deformation of thermally reversible DNA chains versus nanoarchitectures.[5] The tunable thermal reversibility of weak interactions that exists in sticky-end promoted 1-D DNA chains allows the convenient synthesis of free-standing 1-D nanoassemblies.[20−22]

We recently reported the salt-induced hydrophobic self-assembly of the perylenediimide (PDI)-linked DNA dumbbell **D8** (Chart 1), which possesses eight A−T base pairs, into linear aggregates possessing 10−30 monomer units.[8] This dumbbell exists as a monomer in the absence of salt but undergoes association with a rate constant of 3.2×10^7 M^{-1} s^{-1} upon stopped-flow mixing with 0.1 M NaCl. We have also investigated the mechanism of base pair thermal dissociation for a family of PDI dumbbell monomers having 6−16 base pairs (Chart 1).[23] Analysis of the temperature-dependent spectral data provides evidence for a three-state model in which the base pair melting of the intact dumbbell results in the formation of

Received: August 30, 2013
Revised: October 10, 2013
Published: October 22, 2013

ACS Publications © 2013 American Chemical Society

Chart 1. Structures for the Base-Paired Dumbbells D6–D10, D13, and D16 and the Perylenediimide (PDI) Linker

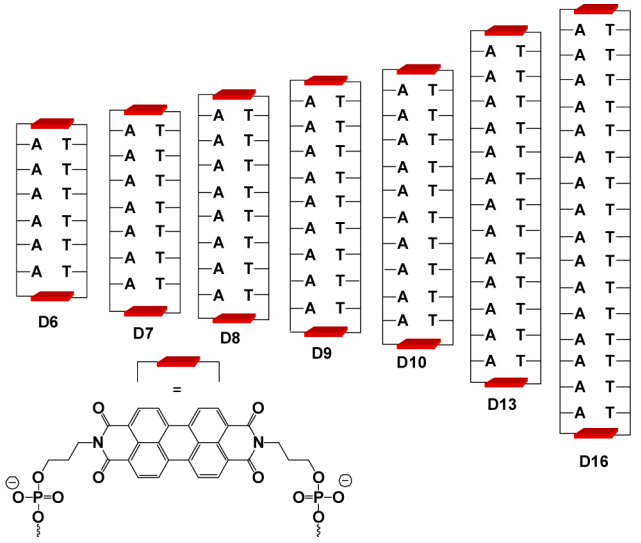

an intermediate species, which is in equilibrium with a collapsed dumbbell having intramolecular PDI–PDI stacking (Scheme 1).

Scheme 1. Three-State Model for Base Pair Dissociation and PDI–PDI Association of Dumbbell D8

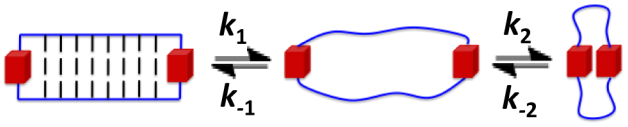

We report here the results of an investigation of the hydrophobic assembly and thermal dissociation of 1-D aggregates formed by the PDI dumbbells in Chart 1 in the presence of NaCl. Both the assembly and the dissociation processes are dependent upon the salt and dumbbell concentrations as well as temperature and the length of the dumbbell. Two limiting mechanisms have been identified for thermal disaggregation. The shorter dumbbells undergo cooperative base-pair and PDI–PDI dimer dissociation, whereas the longer dumbbells undergo sequential PDI–PDI dissociation followed by base pair dissociation. In both cases, the intramolecular dumbbell PDI–PDI association occurs at high temperatures. The mechanistic insight and the precise temperature control of the reversible depolymerization can be beneficial for achieving a predesigned adaptivity in the DNA-based noncovalent polymers.

RESULTS

The synthesis and characterization of dumbbells **D6–10**, **13**, and **16** have been previously described.[23] The long wavelength portion of the UV–vis absorption spectra of conjugate **D13** in 10 mM sodium phosphate buffer in the absence and presence of added NaCl (0.005 to 1.0 M) is shown in Figure 1. The vibronic progression of the long wavelength band in buffer is similar to that of a derivative of the PDI linker that, when dissolved in dichloromethane, has an A^{0-0}/A^{0-1} band intensity ratio of 1.5:1, which is characteristic of nonaggregated PDI derivatives.[24−26] The addition of NaCl results in a red-shift of both the A^{0-0} and the A^{0-1} bands, a decrease in their peak

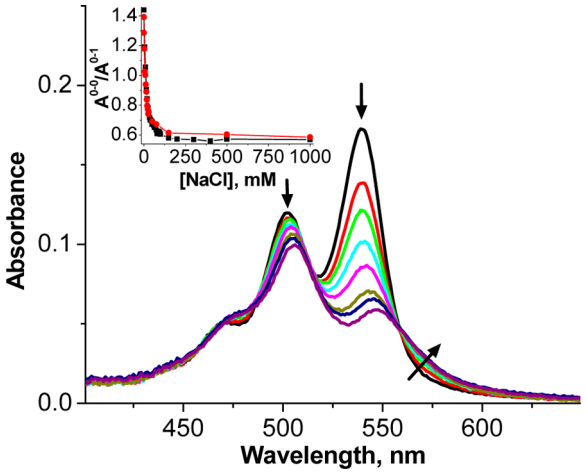

Figure 1. NaCl concentration dependence of the absorption spectra of PDI conjugate **D13** (1 μM) in 10 mM phosphate buffer (pH 7.2). Arrows show the effect of increasing NaCl concentration. Inset shows the ratio of vibronic bands (A^{0-0}/A^{0-1}) of **D13** (red) and **D8** (black) vs the NaCl concentration.

intensities, and a pronounced tailing of the A^{0-0} band toward the long wavelengths. At high salt concentrations the A^{0-0}/A^{0-1} band intensity ratio asymptotically approaches a value of 0.56 at 20 °C, characteristic of dimeric PDI (Figure 1, inset). The effect of added NaCl on the long wavelength band of **D13** is similar to that previously reported for **D8**.[8] The A^{0-0}/A^{0-1} band intensity ratio (1.4:1) in buffer with no NaCl added is independent of the concentration of **D13** (0.5–1.5 μM), indicating that the conjugate is predominantly in the form of the monomer. However, in the presence of 0.1 M NaCl, the band intensity ratio decreases with increasing concentration of **D13** from a value of 0.73 for 0.5 μM **D13** to 0.69 for 1.5 μM **D13** (see Figure S1 of the Supporting Information), indicative of increased aggregation at higher dumbbell concentrations.[8]

The temperature dependence of the absorption spectra of **D13** in buffer without and with 0.1 M NaCl is shown in Figure 2a,c. The 260 nm absorbance increases continuously with increasing temperature, indicative of base pair melting (hypochromism). The A^{0-0} band intensity decreases continuously with increasing temperature in the absence of salt; however, in the presence of salt it first increases and then decreases with increasing temperature. The A^{0-1} band intensity is less sensitive to temperature, both in the absence and the presence of salt. The thermal dissociation profiles obtained from the 260 nm absorption data (A_{260}) and the ratio A^{0-0}/A^{0-1} for 1 μM **D13** in buffer in the absence and presence of 0.1 M NaCl are shown in Figure 2b,d. The profiles obtained in the absence of NaCl have previously been reported.[23] The profiles obtained from the 260 nm absorption data for all of the dumbbells in Chart 1 in the presence of 0.1 M NaCl are shown in Figure 3a. These profiles display a single transition associated with the base-pair dissociation. The first derivatives of these profiles provide the values of T_{260} reported in Table 1 along with the previously reported values of T_{260} obtained in the absence of added salt. The values of T_{260} determined in the presence of 0.1 M salt are strongly dependent upon the dumbbell concentration for the shorter dumbbells but only weakly concentration-dependent for the longer dumbbells (Figure 4). The values of T_{260} for the dumbbells both in the absence and in the presence of 0.1 M NaCl are substantially higher than those of the corresponding T_n:A_n duplexes in the

dx.doi.org/10.1021/jp4087078 | J. Phys. Chem. B 2013, 117, 14649–14654

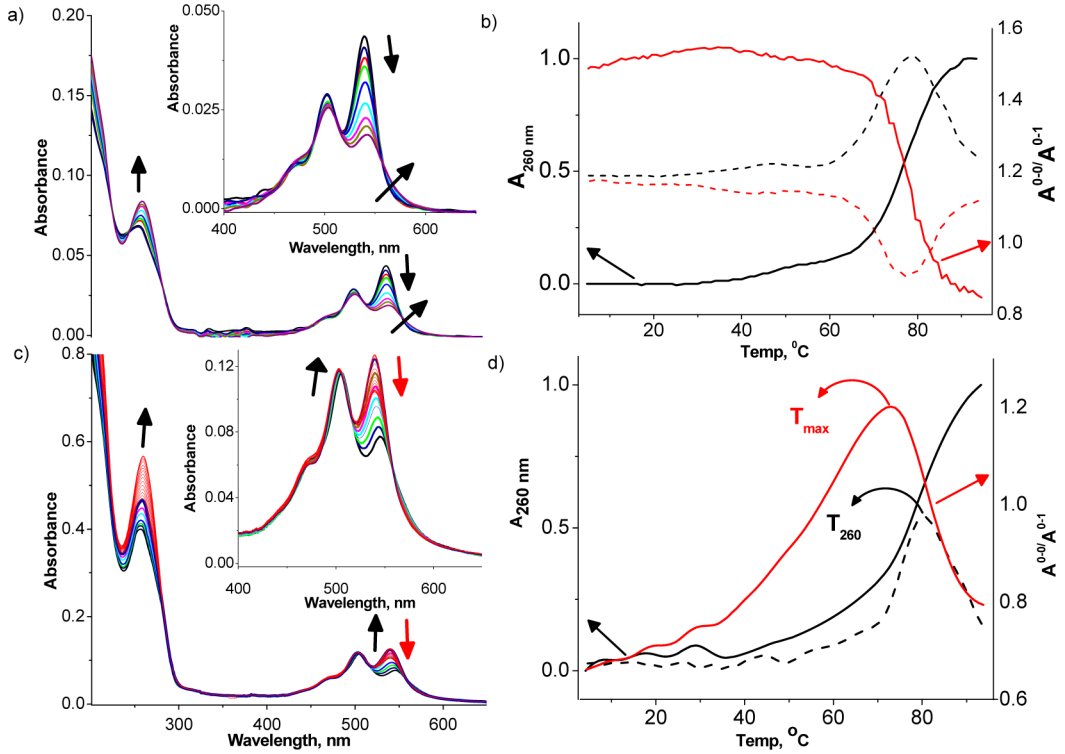

Figure 2. Temperature-dependent absorption spectra of PDI conjugate (a) **D13** (1 μM) in 10 mM phosphate buffer (pH 7.2) and (c) **D13** (2 μM) in 10 mM phosphate buffer (pH 7.2) containing 0.1 M NaCl and thermal profiles for (b) **D13** in 10 mM phosphate buffer (pH 7.2) monitored at 260 nm (left axis) and the ratio A^{0-0}/A^{0-1} (right axis) and (d) in buffer containing 0.1 M NaCl monitored at 260 nm (left axis) and the ratio A^{0-0}/A^{0-1} (right axis). Dashed lines represent the corresponding differential curves.

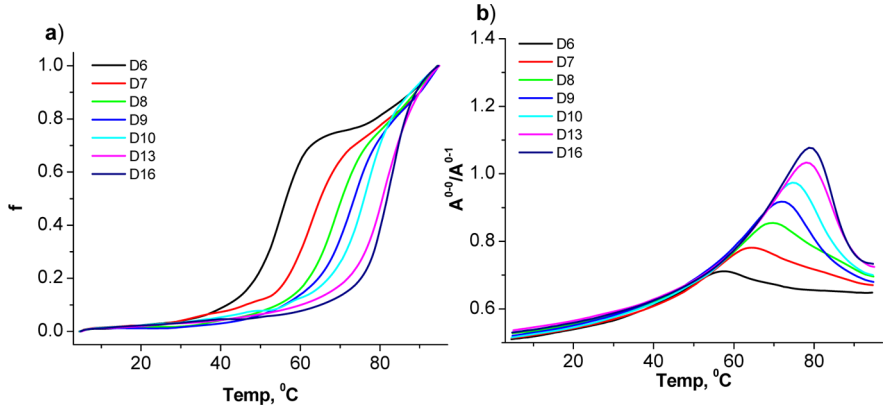

Figure 3. (a) Thermal dissociation profiles obtained at 260 nm for 10 μM solutions of the PDI dumbbell conjugates **D6**–**D10**, **D13**, and **D16** in 10 mM phosphate buffer containing 0.1 M NaCl (f (vertical axis) is the normalized hypochromism). (b) Temperature dependence of the A^{0-0}/A^{0-1} band intensity ratios for 10 μM PDI dumbbell conjugates in 10 mM phosphate buffer containing 0.1 M NaCl.

presence of 0.1 M NaCl. For example the duplex T_8:A_8 has a value of T_m = 17.2 °C under these conditions.

As previously described, a single transition is also observed for the A^{0-0}/A^{0-1} ratio upon heating the dumbbells in buffer in the absence of salt (Figure 2b).[23] The melting temperatures obtained from the first derivatives of these plots (T_{ratio}) are similar to the T_{260} values in buffer (Table 1). The temperature dependence of the A^{0-0}/A^{0-1} ratio in the presence of 0.1 M NaCl is more complex; the ratio first increases to a maximum value at a temperature we define as T_{max} and then decreases upon further heating (Figures 2d and 3b). The initial slopes in Figure 3b are similar for all of the dumbbells for a constant dumbbell concentration, as are the initial values of the A^{0-0}/A^{0-1} ratio at 5 °C (see Figure S2b of the Supporting Information). However, the values of T_{max} (Figure 4 inset), the maximum values of the A^{0-0}/A^{0-1} ratio (see Figure S2a of the Supporting Information), and the values of the A^{0-0}/A^{0-1} ratio at 95 °C (see Figure S2c of the Supporting Information) increase with increasing dumbbell length (Figure 3b). The values of T_{max} (Figure 4, inset) and the A^{0-0}/A^{0-1} ratios at 5 and 95 °C (see Figure S2 of the Supporting Information) also increase with increasing dumbbell concentration for all of the dumbbells.

We have previously reported that the PDI dumbbell **D8** displays, in the absence of salt, a weak monomer emission in buffer and, in the presence of added NaCl, mixtures of monomer and excimer fluorescence with maxima at 549 and 657 nm, respectively.[8] The weak monomer emission is

dx.doi.org/10.1021/jp4087078 | J. Phys. Chem. B 2013, 117, 14649–14654

Table 1. Melting Temperatures for 2 μM Dumbbells in 10 mM Phosphate Buffer[a]

conjugate[b]	$T_{260\ nm}$		T_{ratio}	T_{max}
NaCl, M	0[c]	0.1[d]	0[c]	0.1[d]
D6	42.2	46.2	44.1	47.6
D7	49.5	56.9	50.7	57.1
D8	55.0	63.9	56.2	63.3
D9	69.3	70.5	70.1	65.5
D10	71.8	74.5	72.1	68.4
D13	79.3	78.9	78.2	73.6
D16	80.7	83.0	80.3	75.6

[a]Obtained from the first derivative of the 260 nm thermal dissociation profiles in the presence and absence of 0.1 M NaCl and the A^{0-0}/A^{0-1} ratios in the absence of salt. T_{max} is the temperature at which the A^{0-0}/A^{0-1} ratio attains its maximum value in the presence of 0.1 M NaCl. [b]See Chart 1 for structures. [c]Data from ref 23 obtained in the absence of added salt. [d]Data from present study obtained in the presence of 0.1 M NaCl.

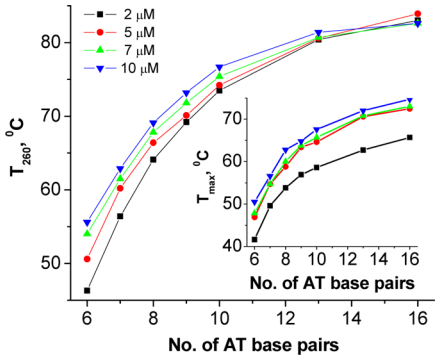

Figure 4. Dependence of melting temperatures T_{260} and T_{max} (inset) on dumbbell length and concentration (2–10 μM) in 10 mM phosphate buffer containing 0.1 M NaCl.

attributed to electron transfer quenching by neighboring adenine bases, and the very weak excimer emission is attributed to the inherently low quantum yield for the PDI-excimer fluorescence. The temperature-dependent fluorescence spectra of 1 μM **D13** in the presence of added 0.1 M NaCl are shown in Figure S3 of the Supporting Information. Increasing temperature results in an increase in the 549 nm monomer intensity. The derivative of a plot of the fluorescence band intensity ratio $I_{549\ nm}/I_{657\ nm}$ (see inset of Figure S3 in the Supporting Information) provides a value of T_{fl} = 80 °C, similar to that obtained from the 260 nm UV melting (Table 1, T_{260}). In the absence of added salt the $I_{549\ nm}/I_{657\ nm}$ band intensity ratio for 1 μM **D13** increases only slightly with increasing temperature indicating that **D13** exists as a monomer under these conditions.

DISCUSSION

The traditional approach to the sticky-end assembly of DNA and RNA nanostructures employs duplexes with relatively short single-strand oligonucleotide overhangs.[6] The thermal dissociation of these nanostructures presumably occurs via a stepwise mechanism with dissociation of the short sticky ends preceding the dissociation of the longer duplex domain. Several years ago, we described the hydrophobic assembly of PDI-linked hairpins into head-to-head hairpin dimers[25,27] and that of PDI-linked dumbbells into linear end-to-end assemblies.[8] These dimers and assemblies are stabilized by the hydrophobic interactions between the PDI sticky ends. Wagenknecht and co-workers have reported the assembly of PDI-capped duplex structures into dimers and 2-D structures.[28−30]

The dumbbells in Chart 1 have values of the A^{0-0}/A^{0-1} band intensity ratio which increase slightly from 0.51 to 0.53 with increasing dumbbell length at a concentration of 10 μM in phosphate buffer containing 0.1 M NaCl at 5 °C (Figure 3b and Supporting Information Figure S2b). These values are comparable to or smaller than those of several PDI dimers,[24,25] in spite of the presence of nondimerized PDI end groups in the linear 1-D dumbbell aggregates. Thus we conclude that, under the conditions of the experiments, as shown in Figure 3 and reported in Table 1, in the presence of 0.1 M NaCl, all of the dumbbells form linear assemblies with average assembly sizes of ≥20 monomers, as previously reported for dumbbell **D8**.[8] The slight increase in the A^{0-0}/A^{0-1} band intensity ratio with dumbbell length can be attributed to the increasing dumbbell monomer solubility as the number of ionic phosphate groups increases.[23] The band intensity ratio also increases as the dumbbell concentration or NaCl concentration decreases, as previously reported for dumbbell **D8**.[8]

The thermal dissociation of the PDI dumbbells is complicated by the intramolecular PDI−PDI dimer formation upon melting of the base pairs separating the two PDI chromophores (Scheme 1). We previously investigated the thermal behavior of these dumbbells in aqueous buffer in the absence of added salt, conditions in which the dumbbells exist largely as monomers.[23] This study permitted the investigation of the base pair dissociation and the intramolecular PDI−PDI association in the absence of the intermolecular PDI−PDI association. The three-state model shown in Scheme 1 was necessary to account for the thermal behavior of the longest dumbbells **D13** and **D16**; however, a two-state model in which the concentration of the intermediate species is very small below 95 °C is adequate to explain the behavior of the shorter dumbbells. The low melting temperatures of the shorter dumbbells in the absence of salt (Table 1) and the low steady state concentration of the intermediate in the three-state model are attributed to the partial compensation of intramolecular PDI−PDI association for the base pair melting of the shorter dumbbells.[23]

The 260 nm thermal dissociation profiles for the dumbbells in 0.1 M NaCl (Figure 3a) display a single transition attributed to base pair melting. The first derivatives of the profiles for 2 μM dumbbell provide the T_{260} values reported in Table 1. Values of T_{260} increase with dumbbell concentration (Figure 4) and are larger in the presence versus absence of NaCl (Table 1), as is normally the case for duplex base pair melting.[31] The values of T_{260} also increase with the number of base pairs (Figure 4) and approach a limiting value for **D16**, also typical of duplex base pair melting.

The A^{0-0}/A^{0-1} band intensity ratio for 2 μM **D13** in the presence of NaCl increases from 0.60 at 5 °C to a maximum value of 1.25 at 64 °C (T_{max}) and then decreases to a value of 0.75 at 95 °C (Figure 3b), indicative of extensive PDI−PDI dissociation at temperatures below 64 °C and reassociation at higher temperature. The plots of the A^{0-0}/A^{0-1} band intensity ratio for all of the dumbbells (10 μM in 0.1 M NaCl) are shown in Figure 3b. These plots have similar initial slopes but differ in both T_{max} (Table 1) and the maximum value of the A^{0-0}/A^{0-1} band intensity ratio (see Figure S2a of the Supporting Information). At temperatures above T_{max} the A^{0-0}/A^{0-1} band intensity ratios decrease with increasing temperature but do not

dx.doi.org/10.1021/jp4087078 | J. Phys. Chem. B 2013, 117, 14649−14654

return to the low values observed at 5 °C (Figure 3b). The values of the A^{0-0}/A^{0-1} ratio at 95 °C at a fixed NaCl and dumbbell concentration increase with increasing chain length (Figure 3b and, in the Supporting Information, Figure S2c). Incomplete base pair melting and the intramolecular PDI−PDI association at 95 °C or poor alignment of the PDI transition dipoles[32,33] can account for the higher values of the A^{0-0}/A^{0-1} ratio for the collapsed dumbbells.

The shapes of the curves in Figure 3b plausibly result from the crossing of a rising curve for the dumbbell disaggregation and a descending curve for the intramolecular PDI association, as shown schematically in Scheme 2.[34] The value of T_{max} is

Scheme 2. Curve Crossing Model for Thermal Behavior of PDI-Linked Dumbbells in 10 mM Phosphate Buffer Containing 0.1 M NaCl (Orange Curve is for D8; the Curves to Right of Scheme are for Longer Dumbbells; the Curves to the Left of Scheme are for Shorter Dumbbells)

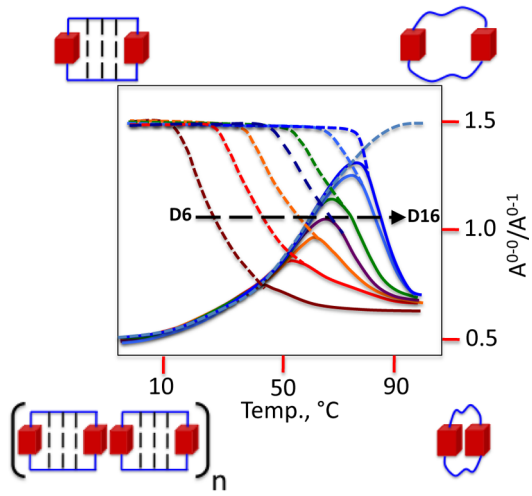

determined by the location of the curve crossing. For **D8** the rising and descending curves cross near the base pair melting temperature, resulting in similar values of T_{max} and T_{260}; however, for the shorter dumbbell **D6** the curves cross slightly above the base pair melting point, resulting in a larger value for T_{max} than for T_{260}, and for longer dumbbells such as **D13** and **D16** the curves cross well below the base pair melting point, resulting in a smaller value for T_{max} than for T_{260} (Table 1). Thus the curve crossing model nicely accounts for the experimental chain length dependence of T_{max} and T_{260} shown in Figure 4 and Table 1. The curve crossing below T_{260} for the longer dumbbells requires that the linear dumbbell aggregates are largely disassembled into monomers prior to the extensive base pair dissociation (Scheme 3a), in accord with the value of $A^{0-0}/A^{0-1} \approx 1.3$ for 2 μM **D16** at T_{max} (Figure S2a of the Supporting Information). Base pair melting then occurs via

Scheme 3. Thermal Behavior of (a) Long and (b) Short PDI-Linked Dumbbells in 10 mM Phosphate Buffer Containing 0.1 M NaCl upon Heating from 5 to 95 °C

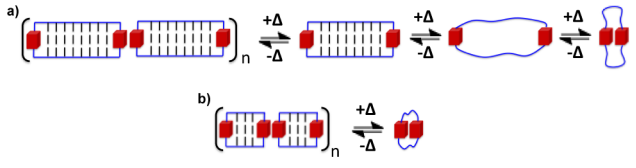

the three-state model previously established for the melting of the longer dumbbell monomers in the absence of salt (Schemes 1 and 3a).[23] Conversely, the curve crossing above T_{260} for the shortest dumbbells requires that disassembly of the linear aggregates, base pair dissociation, and the intramolecular PDI−PDI association occur cooperatively (Scheme 3b).

The thermal behavior of the PDI dumbbells can also be studied using the temperature dependence of the PDI monomer/excimer fluorescence ratio (Figure S3 of the Supporting Information) or circular dichroism spectra (data not shown). However, the information content of these data is inferior to that available from the temperature dependence of the UV−vis absorption spectra and thus is not reported here.

CONCLUDING REMARKS

The thermal response of the PDI-linked dumbbells is complicated by the interplay between inter- and intramolecular PDI−PDI interactions and base pair dissociation. The 1-D dumbbell aggregates are stabilized by the intermolecular hydrophobic PDI−PDI interactions, which are dependent upon the concentration of dumbbell and salt as well as the temperature. The individual dumbbell monomers are stabilized by the PDI linkers at low temperatures, yet intramolecular PDI−PDI association contributes to the dissociation of short dumbbells upon heating.[23] As a consequence of these competing interactions, the aggregates of the longest dumbbells, **D13** and **D16**, disaggregate to monomers prior to extensive base pair melting, whereas the shorter dumbbells undergo cooperative disaggregation and base pair dissociation (Scheme 3). The main parameters that influence this behavior include the hydrophobic/hydrophilic ratio and the DNA length, which allows the tuning of the temperature and the mechanism of supramolecular depolymerization.

The thermal response of the PDI-linked dumbbells can be compared to that of other 1-D DNA sticky-end assemblies. Asanuma and co-workers[9] prepared a series of DNA duplexes possessing 6, 8, or 12 base pairs with mixed base-pair sequences having 5′-ZZZ overhangs, where Z is a covalently linked *p*-methylstilbazole. Assembly occurs via the clustering of two ZZZ overhangs. The melting of the overhangs of the assemblies having 8 or 12 base pairs occurs at lower temperatures than base pair melting, whereas the melting of the overhangs and the base pairs occurs at similar temperatures for assemblies having 6 base pairs. Thus the ZZZ sticky ends are less stable than the longer base pair domains. Conversely, the melting temperatures of the 1-D DNA assemblies based on the β-cyclodextrin-adamantane complexation studied by Chiba et al.[10] have melting temperatures that vary only slightly for duplex lengths of 5−15 base pairs and are higher than those of the corresponding reference duplexes. Thus a range of thermal responses can be observed even for the relatively simple 1-D DNA assemblies having either orthogonal or bis-orthogonal sticky ends.

Recent studies of the thermal response of the DNA nanomaterials including DNA origami,[15,16] nanotubes,[14] and DNA-coated colloids[13] provide evidence for growing interest in the thermal stability and disassembly of DNA nanostructures. The present study of the DNA dumbbells suggests that even the relatively simple 1-D aggregates can have relatively complex thermal behavior that cannot be explained using a simple two-state assembly−dissassembly model. The supramolecular polymers based on such 1D systems can be depolymerized in a controlled manner at specific temperatures, enabling control

dx.doi.org/10.1021/jp4087078 | J. Phys. Chem. B 2013, 117, 14649−14654

over the adaptive properties of the DNA-based noncovalent polymers.

■ ASSOCIATED CONTENT

Supporting Information

UV−vis and fluorescence spectra (Figures S1−S3). This material is available free of charge via the Internet at http://pubs.acs.org.

■ AUTHOR INFORMATION

Corresponding Authors

*E-mail: fdl@northwestern.edu (F. D. L.).
*E-mail: mahesh@iisertvm.ac.in (M. H.).
*E-mail: boris.rybtchinski@weizmann.ac.il (B. R.).

Notes

The authors declare no competing financial interest.

■ ACKNOWLEDGMENTS

This work was supported by grants from the National Science Foundation, Collaborative Research in Chemistry (CHE-0628230 to FDL) and the US−Israel Binational Science Foundation (Grant No. 2010114 to FDL and BR).

■ REFERENCES

(1) Seeman, N. C. DNA in a Material World. *Nature* **2003**, *421*, 427−431.
(2) Wilner, O. I.; Willner, I. Functionalized DNA Nanostructures. *Chem. Rev.* **2012**, *112*, 2528−2556.
(3) Pinheiro, A. V.; Han, D.; Shih, W. M.; Yan, H. Challenges and Opportunities for Structural DNA Nanotechnology. *Nat. Nanotechnol.* **2011**, *6*, 763−772.
(4) Gothelf, K. V.; LaBean, T. H. DNA-Programmed Assembly of Nanostructures. *Org. Biomol. Chem.* **2005**, *3*, 4023−4037.
(5) Castro, C. E.; Kilchherr, F.; Kim, D.-N.; Shiao, E. L.; Wauer, T.; Wortmann, P.; Bathe, M.; Dietz, H. A Primer to Scaffolded DNA Origami. *Nat. Methods* **2011**, *8*, 221−229.
(6) Seeman, N. C. DNA Nanotechnology: Novel DNA Constructions. *Annu. Rev. Biophys. Biomol. Struct.* **1998**, *27*, 225−248.
(7) Yang, H.; Metera, K.; Sleiman, H. F. DNA Modified with Metal Complexes: Applications in the Construction of Higher-Order Metal-DNA Nanostructures. *Coord. Chem. Rev.* **2010**, *254*, 2403.
(8) Neelakandan, P.; Pan, Z.; Hariharan, M.; Zheng, Y.; Rybtchiski, B.; Weissman, H.; Lewis, F. D. Hydrophobic Self-Assembly of a Perylenediimide-Linked DNA Dumbbell into Supramolecular Polymers. *J. Am. Chem. Soc.* **2010**, *132*, 15808−15813.
(9) Kashida, H.; Hayashi, T.; Fujii, T.; Asanuma, H. A Cationic Dye Triplet as a Unique "Glue" That Can Connect Fully Matched Termini of DNA Duplexes. *Chem.—Eur. J.* **2011**, *17*, 2614−2622.
(10) Chiba, J.; Sakai, A.; Yamada, S.; Fujimoto, K.; Inouye, M. A Supramolecular DNA Self-Assembly Based on [Small Beta]-Cyclodextrin-Adamantane Complexation as a Bioorthogonal Sticky End Motif. *Chem. Commun.* **2013**, *49*, 6454−6456.
(11) Rothemund, P. W. K. Folding DNA to Create Nanoscale Shapes and Patterns. *Nature* **2006**, *440*, 297−302.
(12) Kuzyk, A.; Schreiber, R.; Fan, Z.; Pardatscher, G.; Roller, E.-M.; Hogele, A.; Simmel, F. C.; Govorov, A. O.; Liedl, T. DNA-Based Self-Assembly of Chiral Plasmonic Nanostructures with Tailored Optical Response. *Nature* **2012**, *483*, 311−314.
(13) Dreyfus, R. m.; Leunissen, M. E.; Sha, R.; Tkachenko, A.; Seeman, N. C.; Pine, D. J.; Chaikin, P. M. Aggregation-Disaggregation Transition of DNA-Coated Colloids: Experiments and Theory. *Phys. Rev. E: Stat., Nonlinear, Soft Matter Phys.* **2010**, *81*, 041404.
(14) Lo, P. K.; Karam, P.; Aldaye, F. A.; McLaughlin, C. K.; Hamblin, G. D.; Cosa, G.; Sleiman, H. F. Loading and Selective Release of Cargo in DNA Nanotubes with Longitudinal Variation. *Nat. Chem.* **2010**, *2*, 319−328.
(15) Wei, X.; Nangreave, J.; Jiang, S.; Yan, H.; Liu, Y. Mapping the Thermal Behavior of DNA Origami Nanostructures. *J. Am. Chem. Soc.* **2013**, *135*, 6165−6176.
(16) Song, J.; Arbona, J.-M.; Zhang, Z.; Liu, L.; Xie, E.; Elezgaray, J.; Aime, J.-P.; Gothelf, K. V.; Besenbacher, F.; Dong, M. Direct Visualization of Transient Thermal Response of a DNA Origami. *J. Am. Chem. Soc.* **2012**, *134*, 9844−9847.
(17) Lubrich, D.; Green, S. J.; Turberfield, A. J. Kinetically Controlled Self-Assembly of DNA Oligomers. *J. Am. Chem. Soc.* **2009**, *131*, 2422−2423.
(18) Saccà, B.; Niemeyer, C. M. DNA Origami: The Art of Folding DNA. *Angew. Chem., Int. Ed.* **2012**, *51*, 58−66.
(19) Voigt, N. V.; Torring, T.; Rotaru, A.; Jacobsen, M. F.; Ravnsbaek, J. B.; Subramani, R.; Mamdouh, W.; Kjems, J.; Mokhir, A.; Besenbacher, F.; Gothelf, K. V. Single-Molecule Chemical Reactions on DNA Origami. *Nat. Nanotechnol.* **2010**, *5*, 200−203.
(20) Nie, Z.; Petukhova, A.; Kumacheva, E. Properties and Emerging Applications of Self-Assembled Structures Made from Inorganic Nanoparticles. *Nat. Nanotechnol.* **2010**, *5*, 15−25.
(21) Jiang, L.; Sun, Y.; Huo, F.; Zhang, H.; Qin, L.; Li, S.; Chen, X. Free-Standing One-Dimensional Plasmonic Nanostructures. *Nanoscale* **2012**, *4*, 66−75.
(22) Kitching, H.; Shiers, M. J.; Kenyon, A. J.; Parkin, I. P. Self-Assembly of Metallic Nanoparticles into One Dimensional Arrays. *J. Mater. Chem. A* **2013**, *1*, 6985−6999.
(23) Hariharan, M.; Siegmund, K.; Zheng, Y.; Long, H.; Schatz, G. C.; Lewis, F. D. Perylenediimide-Linked DNA Dumbbells: Long-Distance Electronic Interactions and Hydrophobic Assistance of Base-Pair Melting. *J. Phys. Chem. C* **2010**, *114*, 20466−20471.
(24) Giaimo, J. A.; Lockard, J. V.; Sinks, L. E.; Scott, A. M.; Wilson, T. M.; Wasielewski, M. R. Excited Singlet States of Covalently Bound, Cofacial Dimers and Trimers of Perylene-3,4:9,10-Bis(Carboximide)S. *J. Phys. Chem. A* **2008**, *112*, 2322−2330.
(25) Hariharan, M.; Zheng, Y.; Long, H.; Zeidan, T. A.; Schatz, G. C.; Vura-Weis, J.; Wasielewski, M. R.; Zuo, X. B.; Tiede, D. M.; Lewis, F. D. Hydrophobic Dimerization and Thermal Dissociation of Perylenediimide-Linked DNA Hairpins. *J. Am. Chem. Soc.* **2009**, *131*, 5920−5929.
(26) Wilson, T. M.; Zeidan, T. A.; Hariharan, M.; Lewis, F. D.; Wasielewski, M. R. Electron Hopping among Cofacially Stacked Perylenediimides Assembled by Using DNA Hairpins. *Angew. Chem., Int. Ed.* **2010**, *49*, 2385−2388.
(27) Zheng, Y.; Long, H.; Schatz, G. C.; Lewis, F. D. Duplex and Hairpin Dimer Structures for Perylene Diimide-Oligonucleotide Conjugates. *Chem. Commun.* **2005**, 4795−4797.
(28) Baumstark, D.; Wagenknecht, H. A. Perylene Bisimide Dimers as Fluorescent "Glue" for DNA and for Base-Mismatch Detection. *Angew. Chem., Int. Ed.* **2008**, *47*, 2612−2614.
(29) Menacher, F.; Stepanenko, V.; Würthner, F.; Wagenknecht, H.-A. Assembly of DNA Triangles Mediated by Perylene Bisimide Caps. *Chem.—Eur. J.* **2011**, *17*, 6683−6688.
(30) Görl, D.; Zhang, X.; Würthner, F. Molecular Assemblies of Perylene Bisimide Dyes in Water. *Angew. Chem., Int. Ed.* **2012**, *51*, 6328−6348.
(31) Cantor, C. R.; Schimmel, P. R.: *Techniques for the Study of Biological Structure and Function*; W. H. Freeman: New York, 1980; Vol. 2.
(32) Seibt, J.; Marquetand, P.; Engel, V.; Chen, Z.; Dehm, V.; Wurthner, F. On the Geometry Dependence of Molecular Dimer Spectra with an Application to Aggregates of Perylene Bisimide. *Chem. Phys.* **2006**, *328*, 354−362.
(33) Clark, A. E.; Qin, C.; Li, A. D. Q. Beyond Exciton Theory: A Time-Dependent Dft and Franck-Condon Study of Perylene Diimide and Its Chromophoric Dimer. *J. Am. Chem. Soc.* **2007**, *129*, 7586−7595.
(34) Wang, W.; Wan, W.; Zhou, H. H.; Niu, S. Q.; Li, A. D. Q. Alternating DNA and Pi-Conjugated Sequences. Thermophilic Foldable Polymers. *J. Am. Chem. Soc.* **2003**, *125*, 5248−5249.